The Journal of Antibiotics (2016) 69, 843–849

www.nature.com/ja

ORIGINAL ARTICLE

DNA sequence-selective C8-linked pyrrolobenzodiazepine–heterocyclic polyamide conjugates show anti-tubercular-specific activities

Federico Brucoli[1], Juan D Guzman[2,5,6], Mohammad A Basher[3,5], Dimitrios Evangelopoulos[2,4,7], Eleanor McMahon[2], Tulika Munshi[2,8], Timothy D McHugh[4], Keith R Fox[3] and Sanjib Bhakta[2]

New chemotherapeutic agents with novel mechanisms of action are in urgent need to combat the tuberculosis pandemic. A library of 12 C8-linked pyrrolo[2,1-*c*][1,4]benzodiazepine (PBD)–heterocyclic polyamide conjugates (1–12) was evaluated for anti-tubercular activity and DNA sequence selectivity. The PBD conjugates were screened against slow-growing *Mycobacterium bovis* Bacillus Calmette-Guérin and *M. tuberculosis* $H_{37}Rv$, and fast-growing *Escherichia coli, Pseudomonas putida and Rhodococcus sp.* RHA1 bacteria. DNase I footprinting and DNA thermal denaturation experiments were used to determine the molecules' DNA recognition properties. The PBD conjugates were highly selective for the mycobacterial strains and exhibited significant growth inhibitory activity against the pathogenic *M. tuberculosis* $H_{37}Rv$, with compound 4 showing MIC values (MIC = 0.08 mg l^{-1}) similar to those of rifampin and isoniazid. DNase I footprinting results showed that the PBD conjugates with three heterocyclic moieties had enhanced sequence selectivity and produced larger footprints, with distinct cleavage patterns compared with the two-heterocyclic chain PBD conjugates. DNA melting experiments indicated a covalent binding of the PBD conjugates to two AT-rich DNA-duplexes containing either a central GGATCC or GTATAC sequence, and showed that the polyamide chains affect the interactions of the molecules with DNA. The PBD–C8 conjugates tested in this study have a remarkable anti-mycobacterial activity and can be further developed as DNA-targeted anti-tubercular drugs.
The Journal of Antibiotics (2016) **69,** 843–849; doi:10.1038/ja.2016.43; published online 11 May 2016

INTRODUCTION

Tuberculosis (TB) is a global health challenge, with 9 million new cases and 1.5 million deaths reported in 2013.[1] Furthermore, it is estimated that one-third of the world's population is infected with *Mycobacterium tuberculosis*, accounting for a large reservoir of the bacilli.[1] The increasing incidence of TB is also linked to the steady increase in multi-drug- and extensively-drug-resistant TB (MDR/XDR-TB) strains, which renders TB difficult to treat.[1,2] Therefore, new antibiotics with novel and pleiotropic modes of action are urgently needed to combat the TB pandemic, the rise of resistant bacilli and also provide new, safer and shorter drugs regimens. To this end, the complete reconstruction of the *M. tuberculosis* regulatory network[3] has laid the foundation for the development of DNA-targeted anti-mycobacterial agents. The ability of DNA sequence-selective agents to target specific promoter regions of the *M. tuberculosis* DNA can be exploited to disrupt the binding of mycobacterial transcription factors, induce bacterial cell death, overcome antimicrobial resistance and maximize therapeutic efficacy.

DNA-targeted chemotherapeutic agents are an important class of compounds, which have long attracted interest due to their distinctive mode of action involving specific interactions, with predetermined DNA sequences.[4–7] Among these agents, pyrrolo[2,1-*c*][1,4]benzodiazepines (PBDs) have had a major role in cancer and antibacterial chemotherapy.[8,9] PBDs are a family of antitumor-antibiotics first isolated from cultures of *Streptomyces* species.[10] These molecules are DNA sequence-selective agents that covalently bind, via their N10-C11 imine functionality, to the C2-amino groups of guanine residues within the minor groove of DNA, spanning three DNA base pairs with a preference for Pu-G-Pu (where Pu = purine; G = guanine) sequences (Figure 1).[9,11] PBD monomers block transcription by inhibiting RNA polymerase activity in a sequence-specific manner.[12]

[1]School of Sport and Science, Institute of Biomedical and Environmental Health Research (IBEHR), University of the West of Scotland, Paisley, UK; [2]Department of Biological Sciences, Institute of Structural and Molecular Biology, Birkbeck College, University of London, London, UK; [3]Centre for Biological Sciences, University of Southampton, Southampton, UK and [4]Centre for Clinical Microbiology, University College London, London, UK
[5]These authors contributed equally to this work.
[6]Current address: Departamento de Química y Biología, Universidad del Norte, Km 5 vía Puerto Colombia, Barranquilla 081007, Colombia.
[7]Current address: The Francis Crick Institute, Mill Hill Laboratory, The Ridgeway, Mill Hill, London, NW7 1AA, UK.
[8]Current address: Institute of Infection and Immunity, St George's, University of London, Cranmer Terrace, London SW17 0RE, UK.
Correspondence: Dr F Brucoli, School of Sport and Science, Institute of Biomedical and Environmental Health Research (IBEHR), University of the West of Scotland, High Street, Renfrewshire, Paisley PA1 2BE, UK.
E-mail: federico.brucoli@uws.ac.uk
Received 30 September 2015; revised 29 February 2016; accepted 14 March 2016; published online 11 May 2016

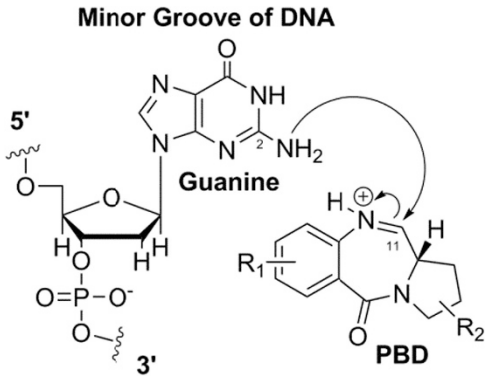

Figure 1 Schematic representation of the mechanism of action of PBDs, involving the nucleophilic attack of the C2–NH_2 group of a guanine residue to the N10-C11 imine moiety of PBD within the DNA minor groove.

Since their discovery, several PBD analogs have been synthesized and extensively evaluated for their anticancer and antibacterial activities.[8,13–17] However, to our knowledge, there are only few studies focusing on the anti-mycobacterial activity of the PBDs. Taylor and Thurston reported that PBD dimers, in which two PBD units are tethered through a C8/C8′′ diether linker to improve DNA-binding affinity and sequence specificity, exhibited notable activity against a panel of rapid and relatively rapid-growing mycobacteria, *Mycobacterium smegmatis*, *M. fortuitum*, *M. abscessus*, *M. phlei* and *M. aurum*.[18] Although showing anti-mycobacterial activity, the PBD dimers displayed significant cytotoxicity against human cell lines, especially compared with PBD monomers, and may be only used as 'drug of last resort' to treat intractable infections caused by multi-drug-resistant pathogens.[19] In another study, Kamal *et al.* showed that PBD-5,11-diones (PBD dilactams) inhibited the growth of *M. avium*, *M. intracellulare* and *M. tuberculosis*. PBD dilactams stabilize duplex DNA to a lesser extent than PBDs, as they lack the N10-C11 imine moiety responsible for the electrophilic alkylation of the C2–NH_2 of guanine bases, thus resulting in a non-covalent DNA interaction and reduced antibacterial and anticancer potency.[9,20]

In the present study, we investigated the anti-mycobacterial activity and DNA-binding properties of a library of 12 C8-linked PBD–heterocyclic polyamide conjugates (**1–12**; Figure 2), which were previously shown to have strong *in vitro* anticancer activities.[21–23] The di- or tri-heterocyclic polyamide chains of **1–12** are comprised of combinations of pyrrole (Py), imidazole (Im) and thiazole (Th) rings known for their ability to modulate the ligands' DNA-binding affinity.[24] C8-linked PBD–polyamide conjugates, unlike PBD dilactams, retain the ability to form covalent DNA adducts, characteristic responsible for their improved cancer cell cytotoxicity and anti-bacterial activities,[15] and have a more favorable cytotoxicity profile compared with the PBD dimers.[15,17]

PBD conjugates **1–12** were screened against slow-growing *M. bovis* BCG and *M. tuberculosis* H_{37}Rv, and fast-growing *Escherichia coli, Pseudomonas putida and Rhodococcus sp.*, and MIC values were determined. Cytotoxicity against mouse macrophages RAW264.7 was also evaluated. The DNase I footprinting experiments and thermal denaturation assays were used to evaluate the DNA recognition properties of **1–12**.

MATERIALS AND METHODS

C8-linked PBD–heterocyclic polyamide conjugates

The 12 PBD conjugates **1–12** were synthesized and purified using published synthetic routes[21,22] and dissolved in dimethyl sulfoxide (DMSO) before use.

Microorganisms and mammalian cells

M. bovis BCG Pasteur (ATCC 35734) and *M. tuberculosis* H_{37}Rv (ATCC 27294), and *E. coli* K12 (ATCC 53323), *P. putida* KT2442 (ATCC 47054) and *Rhodococcus sp.* RHA1 were used to screen the antibacterial activity of the PBD conjugates. Murine macrophages RAW264.7 (ATCC TIB71) were used in this study to evaluate the cytotoxicity of the PBD conjugates.

Mammalian macrophage cytotoxicity assay using resazurin assay

The quantitation of eukaryotic cell toxicity was carried out as previously described.[25]

Antibacterial assay against *E. coli*, *P. putida* and *Rhodococcus sp.*

The evaluation of growth inhibition of the PDB conjugates against *E. coli*, *P. putida* and *Rhodococcus sp.* was performed using the spot culture growth inhibition assay (SPOTi) in 24-well plates.[26] A seed culture of each bacteria was prepared in Luria Bertani (LB) broth and grown overnight at 37 °C, with shaking at 200 r.p.m. *Rhodococcus sp.* was grown in LB broth at 30 °C with shaking at 200 r.p.m. Dilutions of the PBD conjugates were performed in sterile DMSO at concentrations 1000-fold more concentrated than the concentrations to be tested. A measure of 2 µl of each dilution was dispensed in each well of the 24-well plates, and 2 ml of LB agar were added to each well and mixed. A measure of 2 µl of each inoculum containing ~ 10^5 CFUs per ml was carefully dispensed into the middle of the well on the surface of the solidified agar. The plate was incubated overnight at 37 °C for *E. coli* and *P. putida*, and at 30 °C for *Rhodococcus sp.* The plates were visually inspected and MIC values were recorded as the lowest concentration of PBD conjugates, where no growth was observed. Kanamycin was included as positive control.

Anti-mycobacterial screening using high-throughput (HT)-SPOTi

M. bovis BCG and *M. tuberculosis* H_{37}Rv were grown in Middlebrook 7H9 broth supplemented with 0.02% (v/v) glycerol, 0.05% (v/v) Tween-80 and 10% (v/v) albumin, dextrose and catalase (ADC; BD Biosciences, Oxford, UK) as a rolling culture at 2 r.p.m. and 37 °C, and as a stand culture at 37 °C. The anti-mycobacterial activities of the compounds were tested following the HT-SPOTi guidelines.[26,27] HT-SPOTi is a high-throughput growth inhibition assay conducted in a semi-automated 96-well plate format. Compounds dissolved in DMSO at a final concentration of 50 mg ml^{-1} were serially diluted and dispensed in a volume of 2 µl into each well of a 96-well plate to which 200 µl of Middlebrook 7H10 agar medium kept at 55 °C supplemented with 0.05% (v/v) glycerol and 10% (v/v) oleic acid, albumin, dextrose, catalase was added. Wells with no compounds (DMSO only) and isoniazid (positive control) were used as experimental controls. To all the plates, a drop (2 µl) of mycobacterial culture containing 2×10^3 CFUs was spotted in the middle of each well and the plates were incubated at 37 °C for 7 days. The MICs were determined as the lowest concentration of each compound where no mycobacterial growth was observed.

DNase I footprinting assay

Footprinting reactions were performed as previously described[28] using the DNA fragments HexAfor and HexBRev, which together contain all 64 symmetrical hexanucleotide sequences. The DNA fragments were obtained by cutting the parent plasmids with *Hind*III and *Sac*I (*Hex*A) or *Eco*RI and *Pst*I (*Hex*BRev), and were labeled at the 3′-end with [α-^{32}P]dATP using reverse transcriptase. After gel purification, the radiolabelled DNA was dissolved in 10 mM Tris-HCl pH 7.5 containing 0.1 mM EDTA, at a concentration of about 10 c.p.s per µl as determined on a hand held Geiger counter. A measure of 1.5 µl of radiolabelled DNA was mixed with 1.5 µl ligand that had been freshly diluted in 10 mM Tris-HCl pH 7.5, containing 10 mM NaCl. The complexes were left to equilibrate for at least 12 h before digesting with 2 µl DNase I (final concentration about 0.01 units per ml). The reactions were stopped after 1 min by adding 4 µl of formamide containing 10 mM EDTA and bromophenol blue (0.1% w/v). The samples were then heated at 100 °C for 3 min before loading onto 8% denaturing polyacrylamide gels containing 8 M urea. Gels were fixed in 10% acetic acid, transferred to 3MM paper, dried and exposed to a phosphor screen overnight, before analyzing with a typhoon phosporimager.

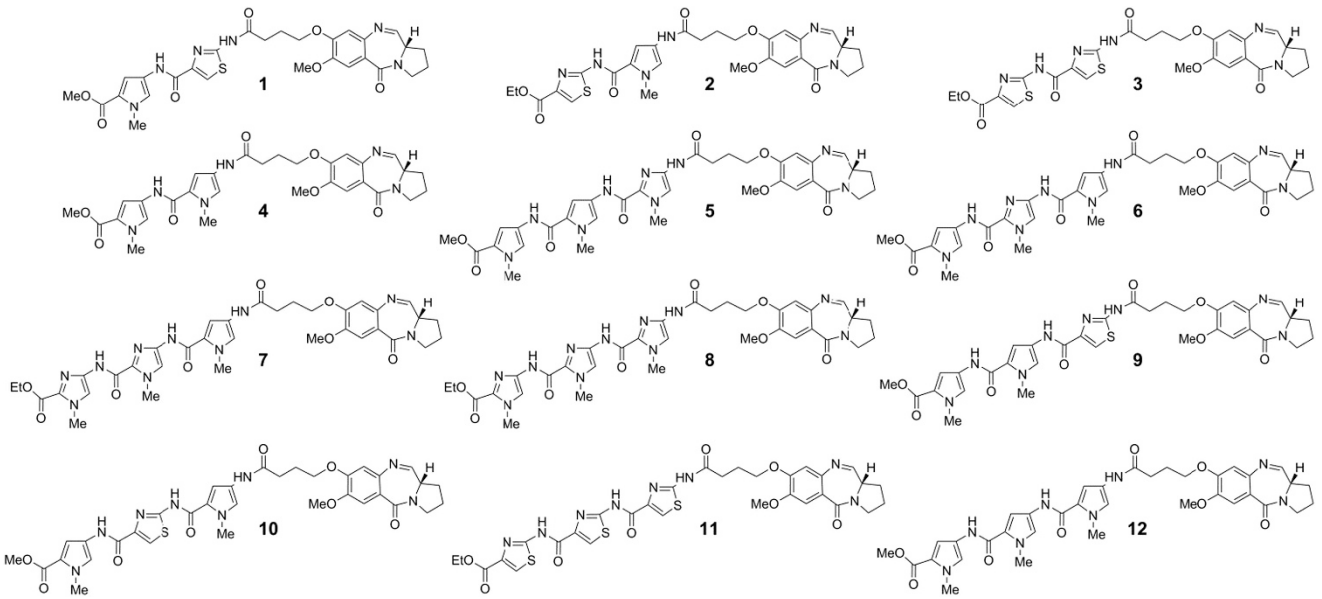

Figure 2 The library of 12 C8-linked PBD–heterocyclic polyamide conjugates **1**–**12** tested in this study.

Table 1 Biological activity of PBD conjugates 1–12

	MICs (mg l^{-1})						
Compound	*Mycobacterium tuberculosis* $H_{37}Rv$	*Mycobacterium bovis* BCG	*Escherichia coli* K12	*Pseudomonas putida* KT2442	*Rhodococcus sp.* RHA1	GIC_{50} RAW264.7 (mg l^{-1})	SI[a]
Py–Th–PBD (**1**)	0.31	0.16	1.25	>20	1.25	4.45	14.4
Th–Py–PBD (**2**)	0.63	0.63	2.5	>50	5.0	2.41	3.83
Th–Th–PBD (**3**)	5.19	<20	>50	>50	>50	2.41	0.46
Py–Py–PBD (**4**)	0.08	0.04	1.25	10.0	1.25	2.41	30.1
Py–Py–Im–PBD (**5**)	0.16	0.16	1.25	10.0	1.25	1.66	10.4
Py–Im–Py–PBD (**6**)	0.32	<20	1.25	50.0	1.25	1.66	5.19
Im–Im–Py–PBD (**7**)	0.16	0.08	1.25	>50	1.25	1.66	10.4
Im–Im–Im–PBD (**8**)	0.32	<20	50.0	>50	10.0	1.66	5.19
Py–Py–Th–PBD (**9**)	0.16	0.08	1.25	50.0	1.25	1.66	10.4
Py–Th–Py–PBD (**10**)	0.16	0.08	1.25	>50	1.25	1.66	10.4
Th–Th–Th–PBD (**11**)	5.19	ND	>50	>50	>50	1.66	0.32
Py–Py–Py–PBD (**12**)	0.16	0.04	1.25	5.0	1.25	1.66	10.4
Isoniazid	0.05	0.05	ND	ND	ND	3000	60 000
Rifampin	0.05	0.05	ND	ND	ND	700	14 000
Kanamycin	ND	ND	1.0	1.0	10.0	ND	ND

Abbreviations: GIC_{50}, half-growth inhibition concentration; ND, not determined; SI, selectivity index.
[a]The SI was calculated by dividing the GIC_{50} for RAW264.7 by the MIC against *M. tuberculosis* $H_{37}Rv$.

DNA thermal denaturation studies

Fluorescence melting curves were determined in a Roche LightCycler (Roche Diagnostics Ltd, Burgess Hill, UK), using a total reaction volume of 20 µl. For each reaction, the final oligonucleotide concentration was 0.25 µM, diluted in 10 mM sodium phosphate pH 7.4 containing 100 mM NaCl. The experiments used the duplexes 5′-F-AAAAGGATCCAAAA/5′-TTTTGGATCCTTTT-Q and 5′-F-AAAAGTATACAAAA/5′-TTTTGTATACTTTT-Q (F = fluorescein and Q = dabcyl). In a typical experiment the samples were first denatured by heating to 95 °C at a rate of 0.1 °C s^{-1}. The samples were then maintained at 95 °C for 5 min before annealing by cooling to 25 °C at 0.1 °C s^{-1} (this is the slowest heating and cooling rate for the LightCycler). They were held at 25 °C for a further 5 min and then melted by heating to 95 °C at 0.1 °C s^{-1}. Recordings of the fluorescence emission at 520 nm were taken during both the melting steps, as well as during annealing. The data were normalized to show the fractional change in fluorescence for each sample between the starting and final values. T_m values were determined from the first derivatives of the melting profiles using the Roche LightCycler software.

RESULTS

Growth inhibition of Mycobacterium spp

In Table 1 are illustrated the results of the anti-tubercular and antibacterial screening, the cytotoxicity evaluation and the selectivity index (SI) of **1–12**. Compounds **1–12** were tested for the growth inhibition against two slow-growing mycobacteria, *M. bovis* BCG and *M. tuberculosis* $H_{37}Rv$. The PBD conjugates' MIC values against *M. tuberculosis* ranged from 0.08 to 5.19 mg l^{-1}, whereas the MIC values against *M. bovis* ranged from 0.04 to 20 mg l^{-1}.

Di-Py-including PBD conjugate **4** (Py–Py–PBD) exhibited the highest growth inhibitory activity against *M. tuberculosis* with a MIC value of 0.08 mg l^{-1}. Compounds **5** (Py–Py–Im–PBD), **7** (Im–Im–Py–PBD), **9** (Py–Py–Th–PBD), **10** (Py–Th–Py–PBD) and **12** (Py–Py–Py–PBD) inhibited the growth of *M. tuberculosis* at 0.16 mg l^{-1} concentration. PBD conjugate **1** (Py–Th–PBD) was active against *M. tuberculosis* and *M. bovis* at 0.31 and 0.16 mg l^{-1}, respectively, whereas compound **2** (Th–Py–PBD) inhibited the growth of both mycobacteria at 0.63 mg l^{-1}. Compounds **6** (Py–Im–Py–PBD) and **8** (Im–Im–Im–PBD) were found to be 60-fold more active against *M. tuberculosis* (0.32 mg l^{-1}) than *M. bovis* BCG (20 mg l^{-1}), whereas PBD conjugates **7**, **9** and **10** were two-fold more active against *M. bovis* (0.08 mg l^{-1}) than *M. tuberculosis* (0.16 mg l^{-1}). Pyrrole-including PBD conjugates **4** and **12** showed the highest growth inhibitory activity against *M. bovis* with a MIC of 0.04 mg l^{-1}. On the other hand, Th-including PBD conjugates **3** (Th–Th–PBD) and **11** (Th–Th–Th–PBD) exhibited the lowest growth inhibitory activity against both *M. tuberculosis* and *M. bovis* BCG with values of 5.19 and 20 mg l^{-1}, respectively. First-line anti-tubercular drugs isoniazid and rifampin were used as positive controls and inhibited the growth of both mycobacterial strains at 0.05 mg l^{-1}.

Antibacterial activity on *E. coli* K12, *P. putida* KT2442 and *Rhodococcus sp.* RHA1

To evaluate the mycobacterial specificity of PBD conjugates **1–12** in whole-cell experiments and determine whether the compounds selectively affected slow-growing mycobacteria in comparison with fast-growing bacteria, we investigated the growth inhibitory activities of **1–12** against Gram-positive *Rhodococcus sp.* RHA1 and Gram-negative *E. coli* K12 and *P. putida* KT2442 bacteria. The results in Table 1 show that the majority of PBD conjugates (**1**, **4–7**, **9**, **10** and **12**) had a significant growth inhibitory activity against *E. coli* and *Rhodococcus sp.* with a MIC value of 1.25 mg l^{-1}. Interestingly, PBD conjugate **8** was 150-fold more active against *M. tuberculosis* (0.32 mg l^{-1}) than Gram-negative *E. coli* and *P. putida* (>50 mg l^{-1}), whereas Th-containing PBD conjugates **3** and **11** were 10-fold more active against *M. tuberculosis* (5.19 mg l^{-1}) than *E. coli*, *P. putida* and *Rhodococcus sp* (>50 mg l^{-1}) strains. Tri-Py-including PBD conjugate **12** was active against *P. putida* at 5 mg l^{-1}, whereas compounds **4** and **5** inhibited the growth of this bacterium at 10 mg l^{-1}. Compounds **7**, **9** and **10** were found to be ~300-fold more active against *M. tuberculosis* (0.16 mg l^{-1}) than *P. putida* (50 mg l^{-1}). The aminoglycoside antibiotic kanamycin was used as a positive control and inhibited the growth of *E. coli* and *P. putida* at 1.0 mg l^{-1} and *Rhodococcus sp.* at 10 mg l^{-1}.

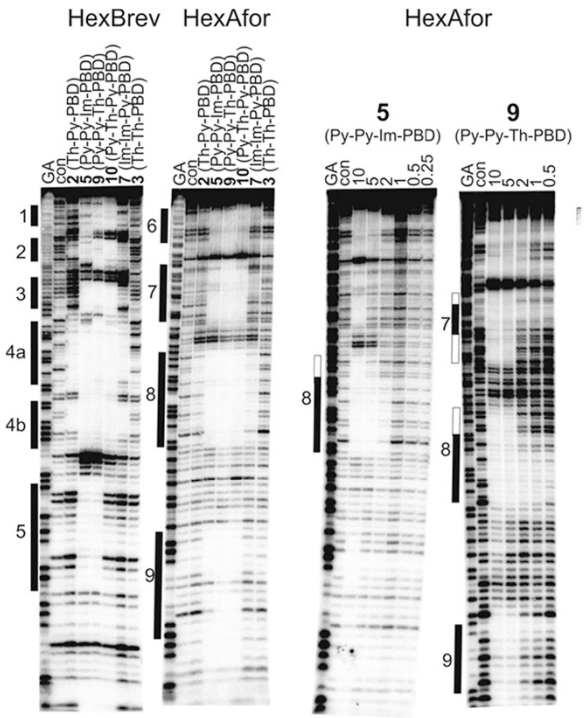

Figure 3 DNase I footprinting patterns of the PBD conjugates on the HexBrev and HexAfor DNA fragments. The first two panels show the results in the presence of 10 μM of each of the PBD conjugates. The second two panels show the concentration dependence of footprints on HexAfor with **5** and **9**. Ligand concentrations (μM) are shown above each gel lane. The bars indicate the location of clear footprints. Tracks labeled GA are sequence markers specific for G and A, although con indicates DNase I cleavage in the absence of added ligand.

Macrophage RAW264.7 cytotoxicity

The PBD conjugates displayed various degrees of cytotoxicity against mammalian macrophages RAW264.7 with half-growth inhibition concentration values ranging from 1.66 to 4.45 mg l^{-1}. The values of the SI, which is the ratio between macrophage half-growth inhibition concentration and MIC against the virulent $H_{37}Rv$ strain, ranged from 0.32 to 30.1, with PBD conjugate **4** (Py–Py–PBD) exhibiting the highest specificity (SI = 30.1) among the library members. PBD conjugates **5**, **7**, **9**, **10** and **12** exhibited a SI of 10.4, whereas **1** had a SI of 14.4. Th-including PBD conjugates **3** and **11** showed the lowest specificity, with SI values of 0.46 and 0.32, respectively.

DNase I footprinting

DNase I footprinting was used to identify the binding sites of the PBD conjugates, using the DNA fragments HexAfor and HexBrev,[28] which together contain all 64 possible symmetrical hexanucleotide sequences. The results are shown in Figure 3. The left hand panels show the footprints with 10 μM of compounds **2**, **3**, **5**, **7**, **9** and **10** with HexAfor and HexBrev, whereas the two panels on the right show examples of the concentration dependence of the footprints with **5** and **9** on HexAfor. It is evident that compounds **5**, **9** and **10** produced large footprints in both HexAfor and HexBrev, whereas compound **7** produced fewer footprints, including two shorter footprints (4a and b) within site 4. Each of these ligands produced a distinct cleavage pattern and the location of the major footprints is indicated in Figure 4. All these compounds contain three rings conjugated to the PBD. A few weaker footprints were seen with the compounds that only contain two conjugated rings. Compound **2**, which contains Th and Py rings, produced footprints at sites 2, 4 and 8, whereas no footprints were seen with **3**, which contains two Th rings. It is clear that the addition of the heterocycles affects the interaction of PBD with DNA. PBD conjugates **5** (Py–Py–Im–PBD), **9** (Py–Py–Th–PBD) and **10** (Py–Th–Py–PBD) bound to sites 1, 2, 3 and 4 within HexBrev, and to sites 6, 7, 8 and 9 within HexAfor, whereas the footprint at site 5 in HexBrev is only evident with compounds **5** and **9**. Compound **7** bound to fewer sites with clear footprints limited to sites 3, 4a and 4b on HexBrev, and site 8 on HexAfor. Although each ligand produced a characteristic cleavage pattern, it is noticeable that many of the footprints contained a short A/T tract followed by a guanine. The two right hand panels of Figure 3 show the concentration dependence of the footprints with **5** and **9** on the HexAfor fragment. At 5 μM

HexBrev
5'-…GGATCCATGCATTAATTCGAATATTGATCATGACGTCGACATGTACATATGTATATACG
1 2

CGCGTACGCGTATACGTAGCGCGCTTATAAGCTTGCAATTGCCGGCTAATTAGGGCCCTC
3 4a 4b

GAGCTCGCGATCGGCCGGATCC-3'
5

HexAfor
5'-…GGATCCCGGGATATCGATATATGGCGCCAAATTTAGCTATAGATCTAGAATTCCGGACC
6

GCGGTTTAAACGTTAACCGGTACCTAGGCCTGCAGCTGCGCATGCTAGCGCTTAAGTACTAG
7 8

TGCACGTGGCCATGGATCC-3'
9

Figure 4 Sequences of HexAfor and HexBrev indicating the location of binding sites of the PBD conjugates (underlined and numbered in sequences). A full color version of this figure is available at *The Journal of Antibiotics* journal online.

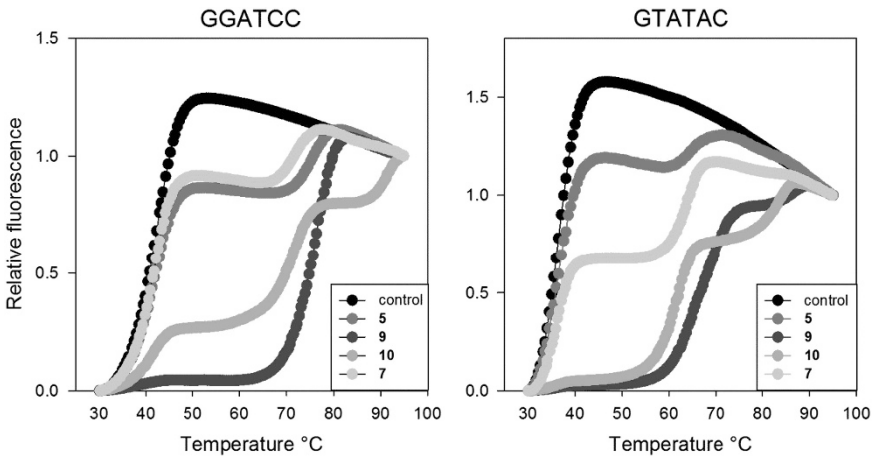

Figure 5 Fluorescence melting profiles for the DNA duplexes 5′-F-AAAAGGATCCAAAA/5′-TTTTGGATCCTTTT-Q and 5′-F-AAAAGTATACAAAA/5′-TTTTGTATACTTTT-Q (F = fluorescein and Q = dabcyl). The ligand concentration was 0.5 μM with 0.25 μM target duplex. A full color version of this figure is available at *The Journal of Antibiotics* journal online.

concentration **5** produced a single footprint located in the lower part of site 8 within the sequence 5′-GCGCTTAAGTACT-3′. Compound **9** produced footprints that persisted to lower concentrations, and the protections at the lower part of site 8 and in the center of site 7 (5′-TAAACGTT-3′) were still evident with 0.5 μM ligand.

DNA melting studies

To further evaluate the contribution of the heterocyclic chains to the DNA recognition properties of the PBD conjugates, the effects of the ligands on DNA melting temperature were analyzed using two fluorescently labeled 14-mer DNA duplexes. These AT-rich DNA duplexes contained either a central GGATCC or GTATAC and the results with 0.5 μM ligand are shown in Figure 5. It can be seen that all four of these ligands stabilised the duplexes and produced transitions at elevated temperatures. As the ligands were covalently attached to the DNA, the T_m values of each transition did not change with the ligand concentration. However, the relative proportions of the different components were altered, so that a greater fraction of the higher T_m was evident with higher ligand concentrations. Each of these duplexes contains more than one guanine with which the conjugates could attach (two guanines for GTATAC and four for GGATCC) and further transitions were observed at higher ligand concentrations, as evident for **10** with both oligonucleotide duplexes. At a concentration of 0.5 μM the ligand was in excess of the target duplex (0.25 μM). The fraction of the melting transition that has shifted to the higher temperature therefore indicates the proportion of the duplex that has been modified within the incubation period, though the absolute values of the melting transitions indicate the stabilization that is imparted by the bound ligand. The result of these experiments are summarized in Table 2. It can be seen that there is a good correlation

Table 2 Changes in melting temperature (ΔT_m) of the oligonucleotide duplexes in the presence of 0.5 μM of each ligand and the fraction of the transition that corresponds to the uncomplexed duplex

	GGATCC T_m = 41.7 °C		*GTATAC* T_m = 36.4 °C	
	ΔT_m °C	*% free*	ΔT_m °C	*% free*
Py–Py–Im–PBD (**5**)	33	75	28	80
Im–Im–Py–PBD (**7**)	30	80	28	55
Py–Py–Th–PBD (**9**)	35	10	29	5
Py–Th–Py–PBD (**10**)	31	25	26	0

between the large footprints produced by PBD conjugates **9** and **10**, with their greatest effect on the melting curves. At 0.5 μM **9** shifted the entire melting curve to a higher temperature with both GTATAC ($\Delta T_m = 29\,°C$) and GGATCC ($\Delta T_m = 35\,°C$) with a small amount of uncomplexed duplex (5% and 10%, respectively). A similar effect is seen with **10** and GTATAC for which ~30% of the transition was shifted to an even higher temperature transition. In contrast, a significant amount of uncomplexed duplex (25%) was still evident with **10** and GGATCC, even though ~20% of the transition corresponded to a higher transition that suggested binding of a second ligand. The melting curves with 0.5 μM **5** and **7** contained a large amount of the transition that corresponded to the uncomplexed duplex. Compounds **5** and **7** had a similar effect on GGATCC, though a greater fraction of GTATAC was bound by **7.**

DISCUSSION

The anti-mycobacterial evaluation of PBD conjugates **1–12** revealed that these compounds have remarkable growth inhibitory activity against *M. tuberculosis* $H_{37}Rv$. The nature and the length of the polyamide chain attached to the PBD unit had a significant influence on the molecules' antimicrobial activity and DNA sequence selectivity. The presence of Py rings in the polyamide chains affected the overall anti-tubercular activity of the compounds. The di-Py-containing **4** had a MIC value of $0.08\,mg\,l^{-1}$, which was comparable with those of isoniazid and rifampin, and an encouraging therapeutic window (SI = 30) that could be further improved in the second generation of PBD-based anti-tuberculosis agents. Although displaying some degrees of cytotoxicity towards mammalian cells, PBD conjugate **4** represents a promising anti-TB therapeutic lead, particularly in light of the results generated by the large TB drug discovery campaign recently conducted by GlaxoSmithKline (Tres Cantos, Madrid, Spain).[29] Researchers at GlaxoSmithKline screened a 2 million proprietary compounds collection for anti-mycobacterial activity against *M. tuberculosis* H37Rv and for cytotoxicity against mammalian cells (HepG2). A set of 177 bioactive leads were identified displaying MIC $< 10\,\mu M$ against H37Rv and selectivity (therapeutic) index ($SI = HepG2IC_{50}/MIC$) > 50. These values are of the same order of magnitude of those displayed by **4** (MIC = 0.13 μM and SI = 30), thus qualifying this compound as a promising lead that can be improved in subsequent medicinal chemistry work.

In addition, compounds **5**, **7**, **9**, **10** and **12**, which exhibited the second best growth inhibitory activity of the series against the TB-causing bacillus ($MIC = 0.16\,mg\,l^{-1}$), all contained at least one Py ring in their three-heterocyclic chains. PBD conjugates with three-Im (**8**) and three-Th (**11**) chains showed a 2-fold and 30-fold decrease in *M. tuberculosis* growth inhibitory activity, respectively. This study also showed that the antimicrobial activity of PBD conjugates **1–12** was highly selective against slow-growing mycobacteria *M. tuberculosis* and *M. bovis* compared with fast-growing bacteria *E. coli*, *P. putida* and *Rhodococcus sp.* The mechanism of action of the PBDs is unique and involves the covalent binding to guanine residues within the DNA minor groove. The DNase I footprinting results showed that the PBD conjugates bound with high affinity to large DNA sequences containing short A/T stretches followed by a guanine residue, with **9** protecting the 5′-TAAACGTT-3′ sequence at a concentration as low as 0.5 μM. This can be exploited to target discrete DNA sequences within the GC-rich mycobacterial genome, and ultimately disrupt key enzymes and transcription factors. DNA melting studies revealed that Th-containing **9**, and to a lesser extent **10**, formed strong complexes and markedly shifted the melting curves of the two 14-mer DNA duplexes used in this study, thus confirming the significant DNA stabilization properties of the compounds. In summary, these results show that **1–12** could serve as DNA-targeted therapeutic leads for the treatment of TB and further studies are underway to implement the potency and therapeutic index of these compounds.

CONFLICT OF INTEREST

The authors declare no conflict of interest.

ACKNOWLEDGEMENTS

We thank Professor Siamon Gordon for providing the RAW264.7 cell line and Professor Simon Croft for granting access to the TB lab in the London School of Hygiene & Tropical Medicine. SB is a Cipla Distinguished Fellow in Pharmaceutical Sciences. Supported by Medical Research Council, UK (grant code: G0801956 to SB) to fund DE and TM's post-doctoral studies at Birkbeck, University of London. JDG received financial support from Colfuturo and a Bloomsbury Colleges studentship for his PhD studies. EM carried out a PhD rotation in SB's lab funded by a Wellcome Trust Scholarship. MAB is a commonwealth scholar in KRF's lab. The funders had no role in the study design, data collection and analysis, decision to publish or preparation of the manuscript.

1 WHO. *Global Tuberculosis Report 2012* (WHO, Geneva, 2014).
2 Guzman, J. D., Gupta, A., Bucar, F., Gibbons, S. & Bhakta, S. Antimycobacterials from natural sources: ancient times, antibiotic era and novel scaffolds. *Front Biosci.* **17**, 1861–1881 (2012).
3 Galagan, J. E. *et al.* The Mycobacterium tuberculosis regulatory network and hypoxia. *Nature* **499**, 178–183 (2013).
4 Denny, W. A. & Abraham, D. J. *In Burger's Medicinal Chemistry and Drug Discovery* (John Wiley & Sons, Inc., 2003).
5 Cozzi, P., Mongelli, N. & Suarato, A. Recent anticancer cytotoxic agents. *Curr. Med. Chem. Anticancer Aagents* **4**, 93–121 (2004).
6 Hartley, J. A. & Hochhauser, D. Small molecule drugs—optimizing DNA damaging agent-based therapeutics. *Curr. Opin. Pharmacol.* **12**, 398–402 (2012).
7 Baraldi, P. G. *et al.* DNA minor groove binders as potential antitumor and antimicrobial agents. *Med. Res. Rev.* **24**, 475–528 (2004).
8 Hartley, J. A. The development of pyrrolobenzodiazepines as antitumour agents. *Expert Opin. Investig. Drugs* **20**, 733–744 (2011).
9 Antonow, D. & Thurston, D. E. Synthesis of DNA-interactive pyrrolo[2,1-c][1,4] benzodiazepines (PBDs). *Chem. Rev.* **111**, 2815–2864 (2011).
10 Leimgruber, W., Stefanovic, V., Schenker, F., Karr, A. & Berger, J. Isolation and characterization of anthramycin, a new antitumor antibiotic. *J. Am. Chem. Soc.* **87**, 5791–5793 (1965).
11 Antonow, D. *et al.* Solution structure of a 2:1 C2-(2-naphthyl) pyrrolo[2,1-c][1,4] benzodiazepine DNA adduct: molecular basis for unexpectedly high DNA helix stabilization. *Biochemistry* **47**, 11818–11829 (2008).
12 Puvvada, M. S. *et al.* Inhibition of bacteriophage T7 RNA polymerase in vitro transcription by DNA-binding pyrrolo[2,1-c][1,4]benzodiazepines. *Biochemistry* **36**, 2478–2484 (1997).
13 Hartley, J. A. *et al.* SG2285, a novel C2-aryl-substituted pyrrolobenzodiazepine dimer prodrug that cross-links DNA and exerts highly potent antitumor activity. *Cancer Res.* **70**, 6849–6858 (2010).
14 Hartley, J. A. *et al.* DNA interstrand cross-linking and in vivo antitumor activity of the extended pyrrolo[2,1-c][1,4]benzodiazepine dimer SG2057. *Investig. New Drugs* **30**, 950–958 (2012)
15 Rahman, K. M. *et al.* Antistaphylococcal activity of DNA-interactive pyrrolobenzodiazepine (PBD) dimers and PBD-biaryl conjugates. *J. Antimicrob. Chemother.* **67**, 1683–1696 (2012).
16 Rosado, H. *et al.* The minor groove-binding agent ELB-21 forms multiple interstrand and intrastrand covalent cross-links with duplex DNA and displays potent bactericidal activity against methicillin-resistant *Staphylococcus aureus*. *J. Antimicrob. Chemother.* **66**, 985–996 (2011)
17 Rahman, K. M. *et al.* GC-targeted C8-Linked pyrrolobenzodiazepine-biaryl conjugates with femtomolar *in vitro* cytotoxicity and *in vivo* antitumor activity in mouse models. *J. Med. Chem.* **56**, 2911–2935 (2013).
18 Hadjivassileva, T., Thurston, D. E. & Taylor, P. W. Pyrrolobenzodiazepine dimers: novel sequence-selective, DNA-interactive, cross-linking agents with activity against Gram-positive bacteria. *J. Antimicrob. Chemother.* **56**, 513–518 (2005).
19 Pepper, C. J., Hambly, R. M., Fegan, C. D., Delavault, P. & Thurston, D. E. The novel sequence-specific DNA cross-linking agent SJG-136 (NSC 694501) has potent and selective in vitro cytotoxicity in human B-cell chronic lymphocytic leukemia cells with evidence of a p53-independent mechanism of cell kill. *Cancer Res.* **64**, 6750–6755 (2004).
20 Antonow, D., Jenkins, T. C., Howard, P. W. & Thurston, D. E. Synthesis of a novel C2-aryl pyrrolo[2,1-c][1,4]benzodiazepine-5,11-dione library: effect of C2-aryl

substitution on cytotoxicity and non-covalent DNA binding. *Bioorg. Med. Chem.* **15**, 3041–3053 (2007).
21 Brucoli, F. *et al.* An extended pyrrolobenzodiazepine-polyamide conjugate with selectivity for a DNA sequence containing the ICB2 transcription factor binding site. *J. Med. Chem.* **56**, 6339–6351 (2013).
22 Brucoli, F. *et al.* Novel C8-linked pyrrolobenzodiazepine (PBD)-heterocycle conjugates that recognize DNA sequences containing an inverted CCAAT box. *Bioorg. Med. Chem. Lett.* **21**, 3780–3783 (2011).
23 Wells, G. *et al.* Design, synthesis, and biophysical and biological evaluation of a series of pyrrolobenzodiazepine-poly(N-methylpyrrole) conjugates. *J. Med. Chem.* **49**, 5442–5461 (2006).
24 Dervan, P. B. Molecular recognition of DNA by small molecules. *Bioorg. Med. Chem.* **9**, 2215–2235 (2001).
25 Brucoli, F. *et al.* Synthesis, anti-mycobacterial activity and DNA sequence-selectivity of a library of biaryl-motifs containing polyamides. *Bioorg. Med. Chem.* **23**, 3705–3711 (2015)
26 Guzman, J. D. *et al.* Antitubercular specific activity of ibuprofen and the other 2-arylpropanoic acids using the HT-SPOTi whole-cell phenotypic assay. *BMJ Open* **3**, e002672 (2013).
27 Danquah, C. A., Maitra, A., Gibbons, S., Faull, J. & Bhakta, S. HT-SPOTi: a rapid drug susceptibility test (dst) to evaluate antibiotic resistance profiles and novel chemicals for anti-infective drug discovery. *Curr. Protoc. Microbiol.* **40**, 17 18 11–17 18 12 (2016).
28 Hampshire, A. J. & Fox, K. R. Preferred binding sites for the bifunctional intercalator TANDEM determined using DNA fragments that contain every symmetrical hexanucleotide sequence. *Anal. Biochem.* **374**, 298–303 (2008).
29 Ballell, L. *et al.* Fueling open-source drug discovery: 177 small-molecule leads against tuberculosis. *Chemmedchem* **8**, 313–321 (2013).